



Effect of fiber type and content on mechanical properties of non-proprietary UHPC concrete

E.Shahrokhinasab¹, D.Garber¹

Department of Civil and Environmental Engineering, Florida International University, Florida, FL, 33174¹



ABSTRACT— The purpose of this study was to investigate the effect of fiber type and content on the mechanical properties of non-proprietary, cost-effective ultra-high-performance concrete (UHPC) mixtures using locally produced material in the state of Florida with crushed limestone fine aggregate. Ultra-fine recovery (UFR) material was used for the first time to improve the particle packing and density of the non-proprietary UHPC mixtures. The UHPC mixes were developed using particle packing analysis and then modified through small trial batches. Qualified mix designs were further evaluated through several different experimental tests, including bulk resistivity. Results showed that using steel fibers with 0.2 mm diameter and 13mm length led to better performance compared to longer metallic fibers and nonmetallic fibers, and less clumping and segregation issues were observed on samples containing these fibers (0.2 mm and 13 mm length). In conclusion, non-proprietary UHPC mix designs containing 2% steel fibers made by locally produced material in Florida, can obtain comparable performance to commercial versions of UHPC mixtures.

KEYWORDS: non-proprietary UHPC, steel fibers, particle packing analysis

1. INTRODUCTION

Today, UHPC concrete has been more popular between academia, engineers, and owners due to its unique properties. High compressive and tensile strength, self-consolidation and exceptional durability, and significant post-cracking ductility are some of the beneficial characteristics of UHPC. UHPC has a higher compressive strength, 151 MPa (22) ksi or higher at 28 days, due to it having a maximum water-to-binder ratio (w/b) of 0.24 [1]. Additionally, low matrix porosity and high particle packing density have given relatively higher durability to UHPC compared to conventional concrete. In terms of chloride diffusion rate, UHPC has shown more than tenfold lower rate compared to conventional concrete and almost zero deterioration rate under freeze and thawing cycles [2], [3]. Adding steel fibers to the mix design results in the UHPC having tensile strengths above 5 MPa (0.72) ksi, and a strain hardening response after initial cracking, and smaller crack widths [4].

These exceptional performance characteristics have made UHPC an ideal option for different parts of the construction industry including precast concrete fields. By enabling designers to choose smaller cross-sections, reduce the conventional reinforcement, increase the prestressing force, and consequently produce longer-span elements, UHPC has made a significant improvement in accelerating the construction process [5].

Adding steel fibers and other materials like silica fume, slag, and superplasticizer, which are usually costly to produce, have increased the average cost of proprietary UHPC 20 times more than conventional concrete. The premium cost of UHPC has limited the widespread use of UHPC in the U.S. infrastructure [4], [6].

To address the high cost of UHPC material, many scholars started developing non-proprietary versions of this

material in different locations around the U.S. This study focused on the effect of fiber type and content on mechanical properties of developed non-proprietary UHPC mixture using locally available material in Florida.

2. Previous Efforts on Developing Non-Proprietary UHPC Concrete

Developing non-proprietary UHPC concrete was noticed initially in Europe around 2009 and a few years later started in the US. There have been several different research efforts, but the first significant one backs to 2013 when the Federal Highway Administration (FHWA) developed non-proprietary UHPC using locally-available materials from Washington, Oregon, North Dakota, South Dakota, New York, and Pennsylvania. Cement, silica fume, and slag were used as binder components, and compressive strengths of 151 to 200 MPa (22 to 29 ksi) were achieved at 28 days [6]. A few years later in 2017 and 2019, fly ash again was used for developing non-proprietary UHPC in Florida and Montana, and in both studies, 124 to 151 MPa (18 to 21 ksi) compressive strengths were achieved [4], [7]. In addition, fly ash, metakaolin, limestone powder, and slag also were used frequently in different research works [2], [8- 11] and led to more than 18 ksi (average) compressive strength at 28 days.

Silica fume was used in most of the previous studies as a major component for developing non-proprietary UHPC concrete. The proportion of cement to silica fume varied mostly between 1.0:0.07 to 1.0:0.25 and the proportion of cement to secondary SCM (slag, fly ash, etc.) was chosen usually between 1.0:0 to 1.0:0.5.

Different water-to-binder ratios from 0.15 to 0.23 were investigated during previous researches, with the ideal ratio depending on the size, type, and distribution of all particles including aggregates and cementitious material [4], [7], [10], [12- 17].

There has been little research trying to use other SCMs like silica powder. One study found that using silica powder did not offer any significant improvement over using silica fume alone [18].

In relation to cement type, a wide variety of cement types have been used for developing non-proprietary UHPC concrete. Considering the price, availability, working time, and 28-days compressive strength of cement paste, Type I/II cement has shown proper performance for developing non-proprietary UHPC, and for this reason, it has been the most frequent used cement type for developing non-proprietary UHPC [6], [4], [19], [12], [9], [13], [10], [14], [11], [2].

3. Research Methodology

Several different raw materials from local manufacturers in Florida were used to develop a non-proprietary UHPC. Initial mix proportions were determined through the particle packing analysis. The initial evaluation of non-proprietary UHPC mix designs was done by casting trial mixtures. This part of the research was completed through small-scale trial batches with a total volume of 0.0042 m³ (0.15 ft³) [20]. Workability of fresh concrete and compressive strength of cylinder samples at different ages were the primary factors for determining the qualified mixtures. The effect of fiber, cement, and aggregate on compressive strength and workability of fresh concrete were initially investigated through small-scale trial tests. Results from these small-scale trial tests were used to guide the mixture designs for the large-scale batches [20].

Nine (9) large-scale mixtures 0.062 m³ (2.2 ft³) were cast to study other properties of non-proprietary UHPC concrete and the effect of different fiber types and content on mechanical properties of non-proprietary UHPC. These mechanical tests included compressive strength, rupture strength, splitting tensile strength,



stiffness (modulus of elasticity), and bulk resistivity.

3.1 Locally Available Materials

Several different materials initially were used for developing non-proprietary UHPC concrete. Most of these materials were locally available like cement (Masonry, Type I-II, and Type III), slag, fine aggregates, and also Ultra Fine Recovery (UFR). UFR is a by-product of batching plants and is still not commercialized for structural uses. It was used in this study to see how it affect the mechanical properties of non-proprietary UHPC. Other materials were purchased from local vendors although the source of material was not from Florida. Two other types of cement also were used in this study.

Table 1 summarizes the information related to all used ingredients in this study.

Material	Details	Sign	Supplier
Fibers	Dramix 4D 65/35BG	A	Bekaert
	Helix 5-13	H	HELIX
	Dramix OL 13/.20	OL	Bekaert
	Hiper Fiber	HF	Hiper Fiber
	STRUX® 90/40	Sy	GCP Applied Technology
Cement	Type M- Masonry Cement	C-M	Titan America
	Type I-II	C-T-I/II	
	Type III	C-T-III	Ash Grove
	Type I-II	C-A-I/II	
	Type I	C-W-I	
Ground-Granulated Blast-Furnace Slag (GGBFS)	-	S	ARGOS USA Cement
Silica Fume	Master Life® SF 10	SF	BASF
Sand	Fine Masonry	FA	Titan America
UFR	-	UFR	Titan America
HRWR	Glenium 7920	HRWR	BASF
VMA	VMA 358	VMA	BASF

Table 1: Material detail, suppliers, and abbreviations [21]

Material	Details	Sign	Supplier
Fibers	Dramix 4D 65/35BG	A	Bekaert
	Helix 5-13	H	HELIX
	Dramix OL 13/.20	OL	Bekaert
	Hiper Fiber	HF	Hiper Fiber
	STRUX® 90/40	Sy	GCP Applied Technology
Cement	Type M- Masonry Cement	C-M	Titan America
	Type I-II	C-T-I/II	
Material	Details	Sign	Supplier
Cement	Type III	C-T-III	Ash Grove
	Type I-II	C-A-I/II	
	Type I	C-W-I	
	Ground-Granulated Blast-Furnace Slag (GGBFS)	-	S
Silica Fume	Master Life® SF 10	SF	BASF
Sand	Fine Masonry	FA	Titan America
UFR	-	UFR	Titan America
HRWR	Glenium 7920	HRWR	BASF

VMA	VMA 358	VMA	BASF
-----	---------	-----	------

3.2 Mix Development

Considering any cementitious mix, two aspects work simultaneously to shape a mix design: the first approach is related to the physical characteristics of constituents and their proportions in the final mix and the second one is related to chemical reactions between cementitious material that produce strong between different used material. These two aspects have to be satisfied fully to get the ideal mix proportions. Particle packing analysis is known as a way to optimize the size distribution of dried constituents to achieve minimum void and a maximum density of mixtures. The required water for chemical reaction between cementitious material was defined through water-to-binder ratio (w/b) which was calculated as the total weight of free water and moisture content of aggregates to the total weight of all used cementitious material in the mixture.

In this study, initial mix proportions were determined through particle packing analysis, and then appropriate water-to-binder ratio (w/b), and dosage of chemical admixtures both techniques were chosen according to the performance of trial batches 0.00425 m³ (0.15ft³).

3.3 Particle Packing Theory

Several different models were used for the particle packing of UHPC by previous research, but the most frequently used method was originally developed by Andreasen and Andreasen [22]. This model later was modified by Funk and Dinger [23] to account for the smallest particle size; this model is shown in (1).

$$D = \frac{D^q - D_{min}^q}{D_{max}^q - D_{min}^q} \quad (1)$$

where:

D(%)	= percent passing for each size
D	= particle size (dimeter)
D _{min}	= minimum used particle size
D _{max}	= maximum particle size
q	= distribution modulus

The distribution modulus (q) is a constant between 0 to 1 which indicates the coarseness of the distribution curve of the mix. A higher distribution modulus indicates more coarsely graded mixtures. Most of the previous studies used values between 0.19 to 0.37 according the distribution size of initial constituents [2], [9], [12], [24].

3.4 Particle Packing Analysis

The first step of particle packing analysis is to provide an accurate full distribution curve of the constituent materials. The distribution curves of the different components used in the mixture were determined through different laboratory techniques. To get an accurate distribution curve of components, both the physical sieving method (for coarser particles) and an image processing method for fine particles (less than 1000µm) were used. Image processing was done using a laser diffraction device (Malvern Mastersizer 2000). The particle size distributions of all used dry materials in this study are shown in Figure 1 (a).

The ideal curve was determined according to (1) and considering the minimum and maximum particle size

which is shown in both Figure 1 (a) and (b). Figure 1 (b) shows the sensitivity of the ideal curve to the distribution modulus (q). In this study, q of 0.25 was used for determining the ideal curve according to previous research [2], [9], [11].

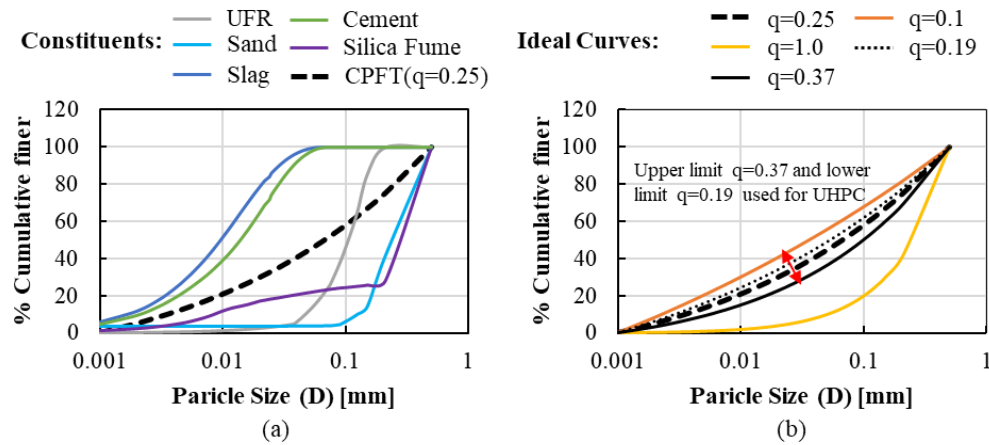


Figure 1: (a) Particle size distribution of different constituents and (b) Ideal curve according modified Andreasen and Andersen model considering different q values ($D_{max} = 0.5$ mm and $D_{min} = 0.001$ mm). [21]

3.5 Qualified UHPC Mixtures

The ideal curve theoretically defines a mixture with minimum void and maximum density. A distribution curve close to the ideal curve represents higher density and lower void compared to other mixtures, which results in higher strength and lower permeability. A spreadsheet was developed to determine mixture proportions with minimum distance from the ideal curve. Numerous mixture proportions were evaluated through the developed spreadsheet; five of these mixtures with different amounts of UFR were chosen for further investigation. The distribution curves of these mixture proportions and the ideal curve with a distribution modulus of 0.25 are shown in Figure 2.

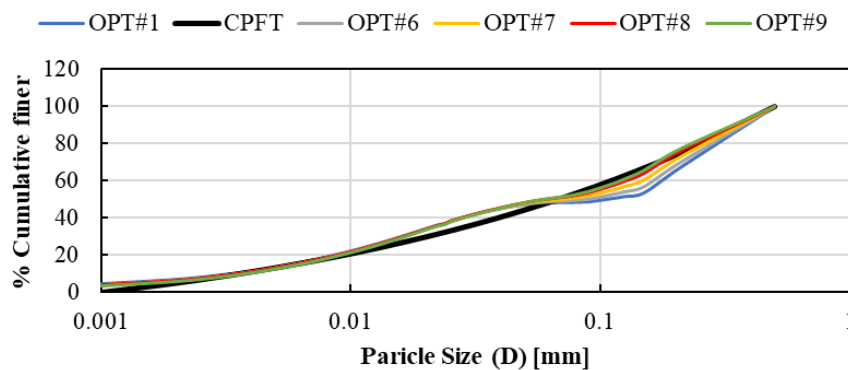


Figure 2: Particle size distribution of qualified mix proportions and ideal distribution curve with $q= 0.25$

Details of these mixture proportion are provided in Table 2. The main difference between these mixture proportions was the replacement portion of sand with UFR. Particle packing analysis revealed that replacing the sand with UFR (up to 35%) improves the distribution curve compared to the mixture without UFR (OPT#1). UFR, with its very small particle size, can fill the gap between coarser particles and increase the density of the mixture.

Table 2: Proportions of the initially qualified mixes

Mixes	Agg./C	Cement Slag Silica Fume			Sand	UFR
		Cementitious Materials				
OPT#1	1.0	0.6	0.3	0.1	1.00	0.00
OPT#6	1.0	0.6	0.3	0.1	0.90	0.10
OPT#7	1.0	0.6	0.3	0.1	0.80	0.20
OPT#8	1.0	0.6	0.3	0.1	0.70	0.30
OPT#9	1.0	0.6	0.3	0.1	0.65	0.35

OPT#1 and OPT#6 to OPT#9 were chosen for further investigation in large-scale batches. The proper dosage of high range water reducers and proper water to binder ratio were determined through small-scale trial batches with total volume of 0.004 m³ (0.15ft³) [20] and were modified as needed to keep the desired flowability.

4. Large-Scale Experimental

Based on observations during the trial batches, nine different mixture designs were considered for further evaluation of non-proprietary UHPC concrete. These mixtures had proportions based on the findings from the small-scale batches [20]. Table 3 summarizes the mix proportion of nine qualified large-scale mixture designs. The w/b value represents the total weight of water and water content of aggregates to the weight of all cementitious material.

Table 3: Specification of large-scale batches

Mix.	Fiber Type	Vol. %	w/b	Agg./b	C	Slag	SF	Sand	UFR	Cement Type	Glenium (oz/cwt)	VMA (oz/cwt)
L1	OL	2	0.20	1.00	0.60	0.30	0.10	0.7	0.3	C-T-I/II	29.4	0.00
L3	OL	2	0.20	1.00	0.60	0.30	0.10	1.0	0.0	C-T-I/II	27.5	0.00
L4	OL	2	0.18	1.00	0.60	0.30	0.10	1.0	0.0	C-T-I/II	27.5	0.00
L5	HF	2	0.20	1.00	0.60	0.30	0.10	1.0	0.0	C-T-I/II	27.5	0.00
L6	A	1.5	0.20	1.00	0.60	0.30	0.10	1.0	0.0	C-T-I/II	27.5	4.49
L7	OL	4	0.20	1.00	0.60	0.30	0.10	1.0	0.0	C-T-I/II	27.5	0.00
L8	HF	4	0.20	1.00	0.60	0.30	0.10	1.0	0.0	C-T-I/II	27.5	0.00
L9	Sy	2	0.20	1.00	0.60	0.30	0.10	1.0	0.0	C-T-I/II	27.5	0.00
L10	Sy	1	0.20	1.00	0.60	0.30	0.10	1.0	0.0	C-T-I/II	27.5	0.00

The following variables were evaluated using these nine different mixture designs:

- Fiber type and content (Comparing L3 and L5 to L10)
- UFR content (comparison between L1 and L3)
- w/b Ratio (comparison between L3 and L4)

All nine mixtures were cast using an Imer Mortarman vertical shaft paddle mixer (MIX 750 MBP) with 0.062 m³ (2.2-ft³) volume. The entire mixing process took between 20 to 30 minutes, consisting of 10 minutes of mixing dry components (except fiber) and 10 to 20 minutes of mixing after adding water and chemical admixtures. This time varied based on the specific mixture proportions, materials, and mixing energy provided by the paddle mixer. Mixing times should be tested through trial batches before casting any large volume of UHPC. The fibers were then gradually added during the last 5 minutes of the mixing process to avoid any fiber clumping issue.

From each large mixture, 36 76.2 mm by 152.4 mm (3-in. by 6-in.) cylinders, 4 101.6 mm by 203.2 mm (4-in.



by 8-in.) cylinders, 3 152.4 mm by 304.8 mm (6-in. by 12-in.) cylinders, and 5 76.2mm by 76.2mm by 279.4mm (3-in. by 3-in. by 11-in.) prisms were cast.

Two different tests were conducted on fresh non-proprietary UHPC and five tests were used to evaluate the mechanical properties of hardened samples, based on the availability of equipment. A summary of the tests used in this study is shown in Table 4.

Table 4: Conducted tests for qualified UHPC mixtures [25- 33]

Property	Test Method	Age for Testing (# specimens tested)
Flowability	ASTM C1437 ASTM C230	tested during casting
Set Time	ASTM C403	at time of casting (3)
Compressive Strength	ASTM C39 ASTM C1856	3 days (3), 28 days (3)
Modulus of Elasticity	ASTM C469 ASTM C1856	28 days (3)
Splitting Tensile Strength	ASTM C496	28 days (3)
Modulus of Rupture	ASTM C78	28 days (3)
Bulk Resistivity Test	ASTM C1760	3,7,14,28,56 and 90 days (4)

Half of the samples for compressive strength, modulus of elasticity, and splitting tensile strength were stored in a lime water bath 24 hours after casting until test day to investigate the effect of moist curing. The rest of the samples were stored in a temperature-controlled room until they were demolded 24 hours before testing.

5. Discussion of Results

5.1 Effect of fiber type and content

The effect of fiber type and content was investigated by comparing the results of experimental tests for L3 and L5 to L10 mixtures. Setting time is defined by the period of time required for the fresh concrete to reach to a certain level of consistency which usually is measured by penetrating different standard needles to the fresh concrete. The resistance stress versus time for the mixtures with different fiber types and fiber contents are shown in Figure 3.

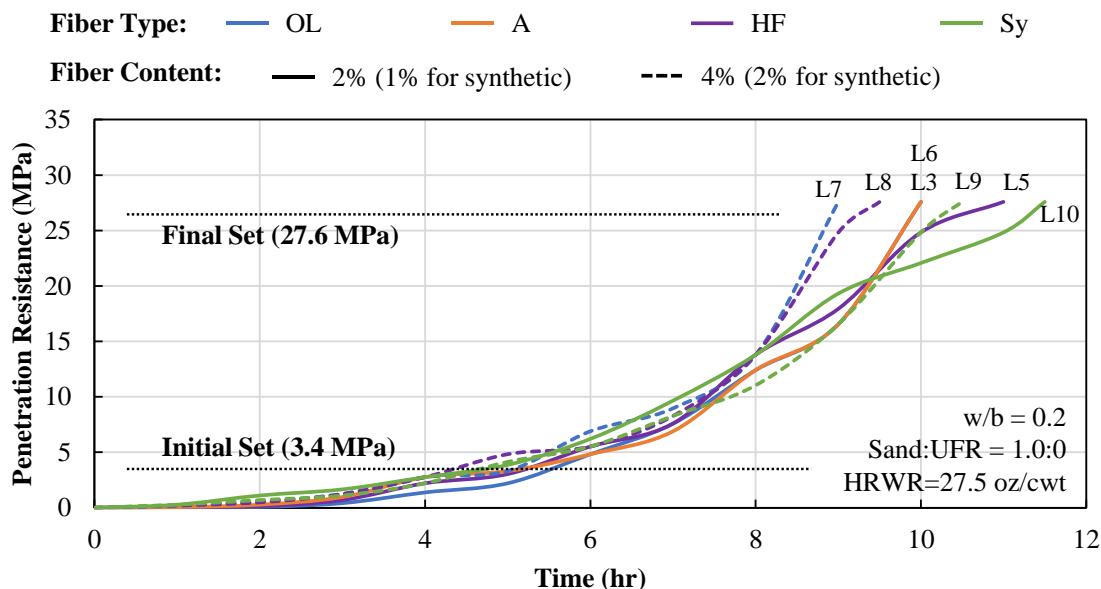


Figure 3: Effect of fiber type and content on setting time

A higher fiber content was found to lead to a shorter setting time, seen by comparing L7 and L8 (4% steel fiber content) with L3, L6, and L5 (2% steel fiber content) shown in Figure 3. This observation can be explained by the more resistance of penetration due to the higher probability of encountering the penetration needles by fibers. As it is shown schematically in Figure 4, in mixtures with higher fiber content, the chance of encountering needles by fibers is higher than mixtures with lower fiber content. There was no clear correlation between fiber type and setting time; all mixtures with 2% fibers had similar setting times.

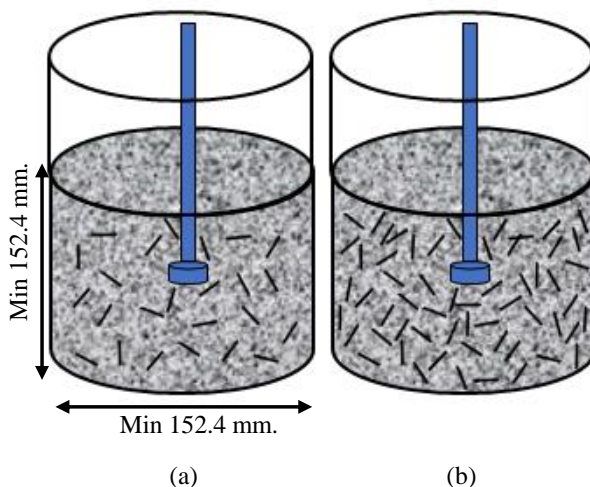


Figure 4: Schematic of setting time test; (a) low volume content fibers and (b) high volume content

Figure 5 (a) and (b) shows the average measured compressive strength and density of L3 and L5 to L10 mixtures. No clear relationship was observed between fiber content and compressive strength, but fibers with higher content showed a 3 to 4% increase in the average measured density of samples.

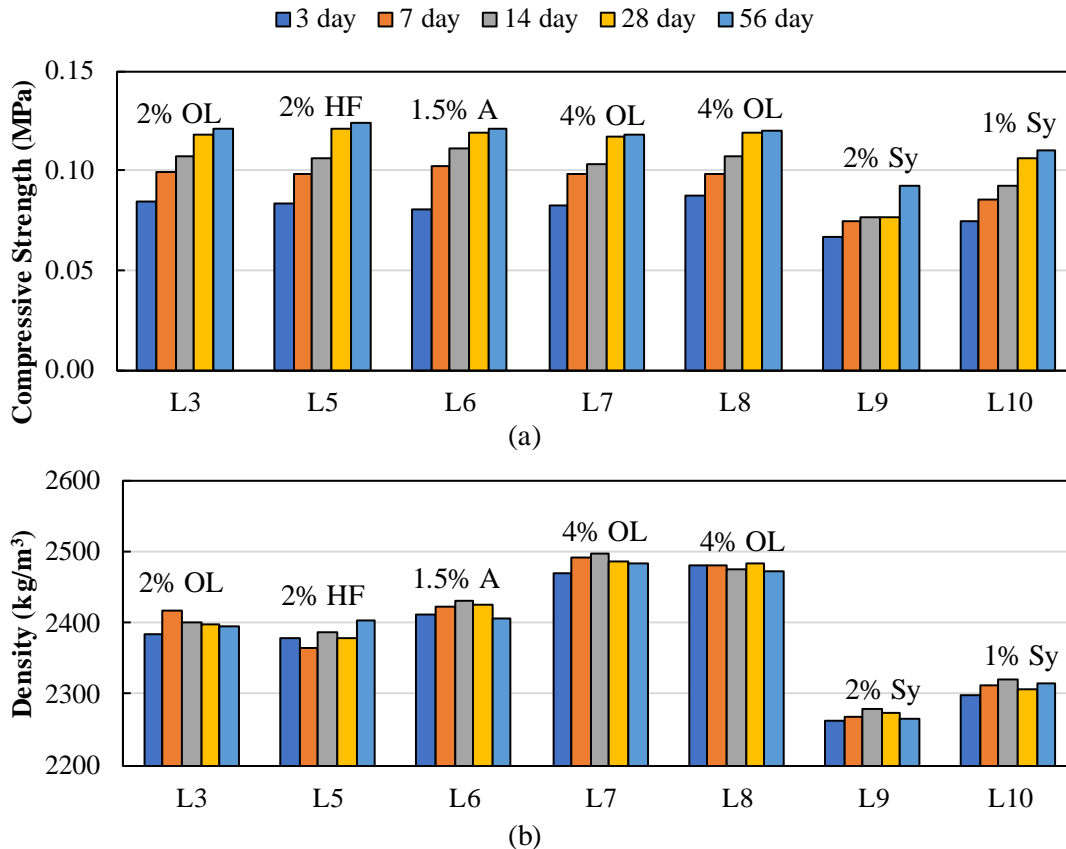


Figure 5: Effect of fiber type and content on (a) compressive strength and (b) density

Also, results showed that the mixtures containing synthetic fibers had lower compressive strength and density compared to the mixtures made with steel fibers. This low compressive strength initially was likely due to the lower strength of the synthetic fibers themselves compared to steel fibers. There were also some observed fiber clumps in mixtures containing synthetic fibers, which may have also contributed to the low compressive strength of mixtures made with synthetic fibers. Fiber clumping was also observed in some samples with long steel fibers with anchored ends (L6, 1.5% A fibers), but these samples had similar compressive strengths to other samples with steel fibers.

The modulus of elasticity of mixtures was calculated according to stress-strain curve and mentioned provisions ASTM C469 and ASTM C1856. Figure 6 (a) shows the calculated modulus of elasticity for each mixture according to curing condition. The measured modulus of elasticity of taken samples was between 48,952 and 65,500 MPa (7,100 and 9,500 ksi), which was in the same range for UHPC (29300 to 55,158 MPa or 4,250 to 8,000 ksi) found by previous researchers [34].

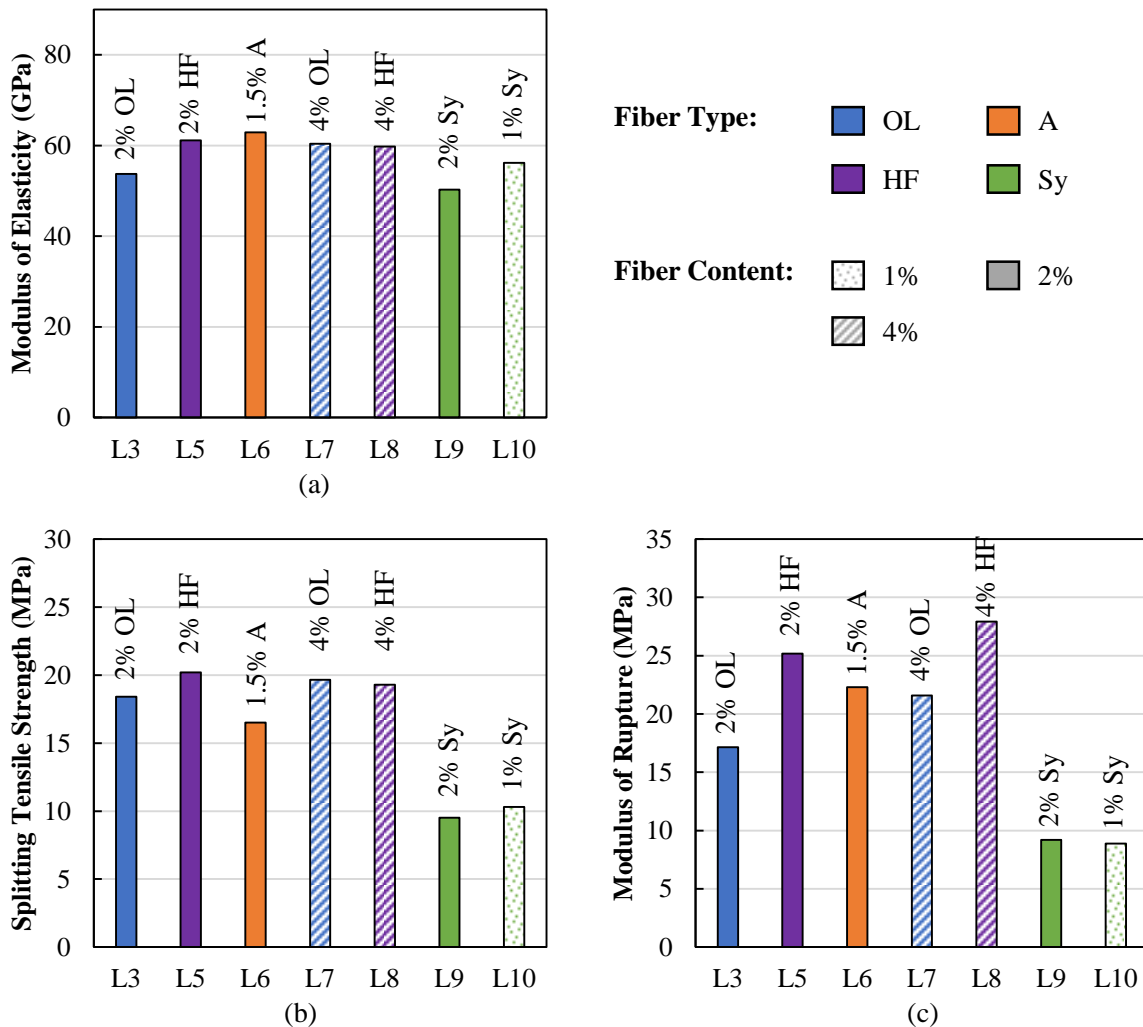


Figure 6: Average (a) modulus of elasticity, (b) splitting tensile, and (c) modulus of rupture for L3 and L5 to L10 mixtures

Comparing L3 and L7 shows around a 12% increase for modulus of elasticity by increasing the fiber content from 2 to 4% with OL fibers, while the same comparison between L5 and L8 with HF fibers indicates only a 2% increase of modulus of elasticity by increasing the fiber content from 2 to 4%. This trend was opposite for mixtures containing synthetic fibers and revealed an 11% decrease in measured modulus of elasticity by increasing the fiber content from 1 to 2%. Comparing steel to synthetic fibers, it was observed that the use of steel fibers resulted in a stiffer UHPC than using synthetic fibers.

Results of the splitting tensile strength test are shown in Figure 6 (b). L9 and L10 containing synthetic fibers showed the lowest splitting tensile strength while L5 containing 2% HF fibers showed the highest splitting tensile strength between all other mixtures. Mixtures containing synthetic fibers showed on average 47% lower splitting tensile strength than mixtures containing steel fibers.

Splitting tensile strength increased slightly with increasing fiber content for OL fibers but decreased with increasing fiber content for both HF and synthetic fibers. The observed results did not show any clear relationship between fiber type and content and splitting tensile strength. The A fibers showed lower splitting tensile strength compared to other mixtures made with steel fibers but still showed higher strength than

mixtures containing synthetic fibers.

Modulus of rupture was the last mechanical test that was conducted over samples taken from large-scale mixtures. Results of this test are shown in Figure 6 (c) for mixture L3 and L5 to L10. Results showed that increasing the fiber content from 2% to 4% increased the modulus of rupture for OL, HF, and synthetic fibers by approximately 26%, 11%, and 4%, respectively. A higher modulus of rupture strength was observed for mixtures with HF fibers compared to OL fibers. Comparing L3 and L5 with 2% fiber content showed 47% increase of modulus of rupture for HF fibers compared to OL fibers, and comparing the L7 and L8 with 4% fiber content revealed 30% increase for HF fibers compared to OL fibers. Mixtures made with synthetic fibers showed the lowest measured modulus of rupture in the group which was approximately half of the MOR for the batches with 2 percent OL fibers.

Figure 7 also shows the average flexural stress versus displacement curves of the mixture L3 and L5 to L10. Peak points on these curves represent the average peak flexural stress of mixtures. Considering the shape of curves represent an after cracking flexural behavior of fiber reinforced concrete which is much different than the typical behavior of normal concrete which accompanies by immediate failure after cracking.

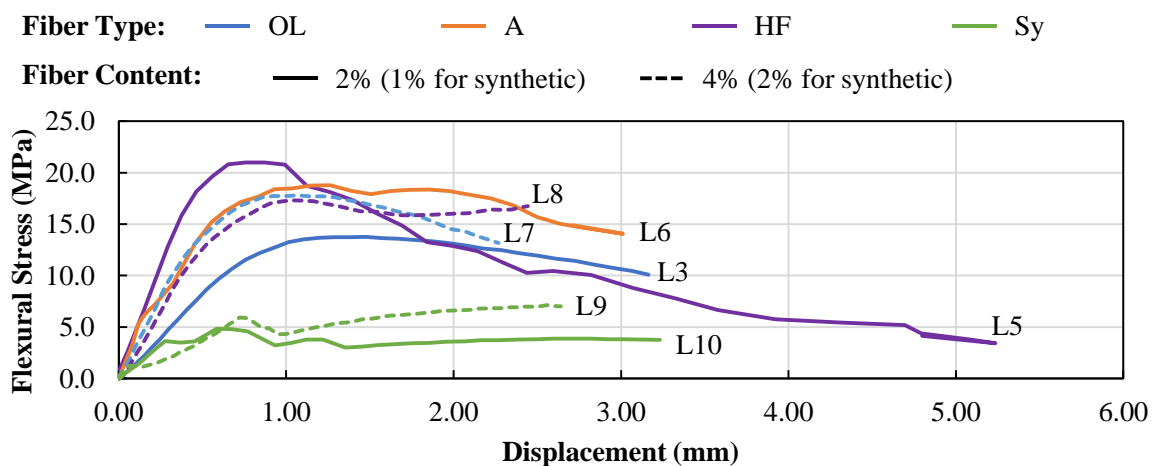


Figure 7: Flexural stress versus midspan displacement curves for samples investigating the effect of fiber type and content on the modulus of rupture

5.2 Effect of using Ultra Fine Recovery (UFR) and w/b

UFR was used in this study to evaluate its effect on the mechanical properties of UHPC mixtures. Figure 8 shows the setting time of L1, L3, and L4 mixtures. As it was expected, results showed that a lower w/b ratio led to a shorter setting time. Besides, results showed that the mixture containing 30% UFR had a slightly longer setting time; this could be also due to higher HRWR content and not necessarily the effect of using UFR.

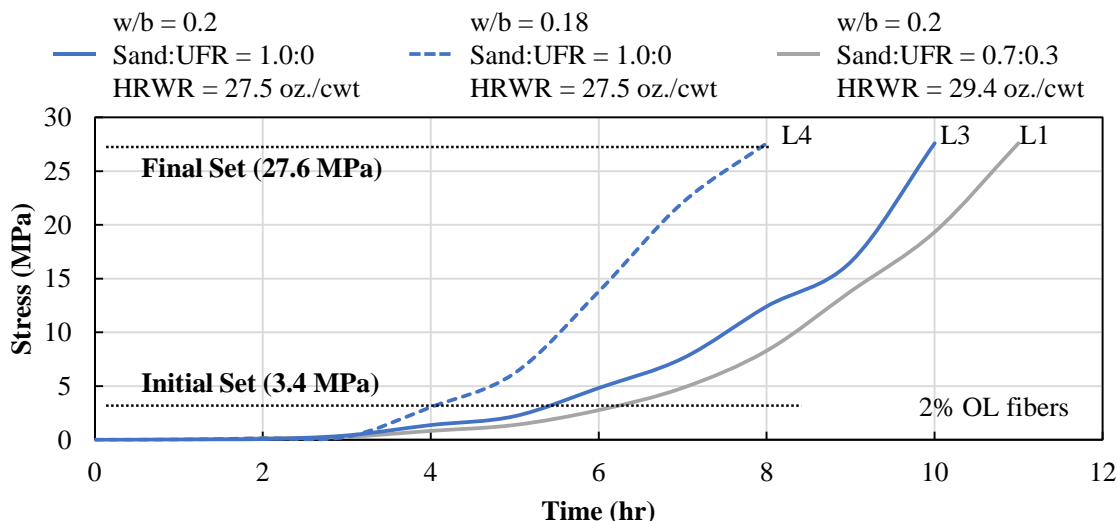


Figure 8: Effect of w/b and UFR on setting time

The measured compressive strength and density of L1, L3, and L4 mixtures are shown in Figure 9. As UFR was effective for improving the particle packing, higher density and probably higher compressive strength could be expected, but results showed slightly lower compressive strength of mixture containing UFR compared to the mixture without UFR, and also density did not change significantly. Although this result did not show any significant improvement of compressive strength and density, but it was found effective during the small trial batches. The reason for this variation in results is not clear and requires more investigations on using UFR. On the other hand, using a lower w/b ratio (0.18) was effective and led to increasing of compressive strength between 2 to 6 percent at different ages.

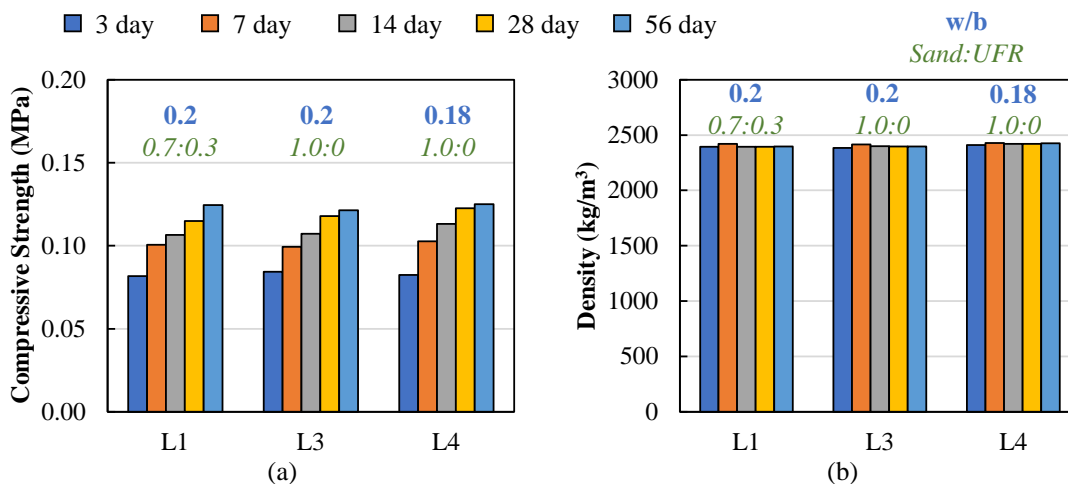


Figure 9: Effect w/b and UFR on (a) compressive strength and (b) density

The measured average modulus of elasticities for L1, L3, and L4 mixtures are shown in Figure 10 (a). Using UFR was found effective and samples containing UFR (L1) had an average 12.5 percent higher modulus of elasticity than samples made by only masonry sand (L3). Besides, decreasing w/b from 0.2 to 0.18 showed on average 17.3 percent higher modulus of elasticity.

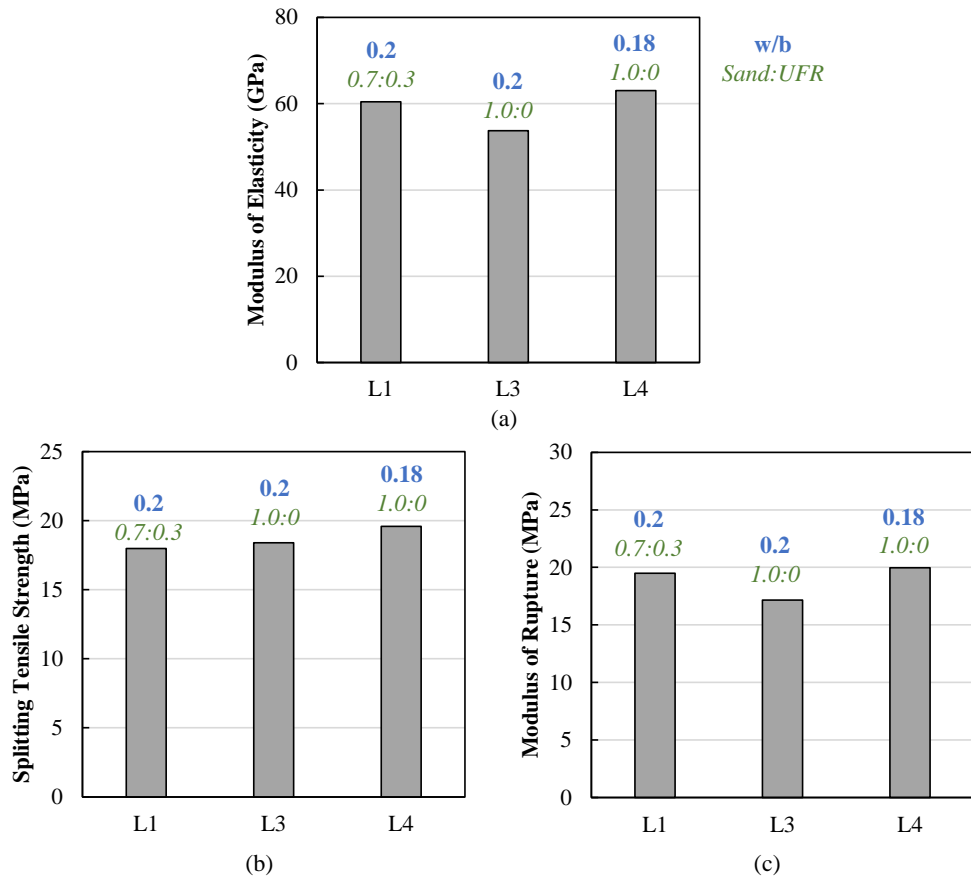


Figure 10: Effect of w/b and UFR on the (a) modulus of elasticity, (b) splitting tensile strength, and (c) modulus of rupture

The results of the splitting tensile strength test for L1, L3, and L4 mixtures are shown in Figure 10 (b). Decreasing the w/b ratio from 0.2 to 0.18 was found effective and led to 6% increase in splitting tensile strength while using UFR made a slight decrease in splitting tensile strength. The lower splitting tensile strength of L1 compared to L3, could be due to slightly higher dosage of HRWR and not because of using UFR. The liquid portion of chemical mixtures like HRWR acts like water and can change the previously determined w/b. The most accurate way of measuring w/b is to consider the free water, moisture content of aggregate, and also the liquid portion of all chemical admixtures altogether. This can explain why in several cases using UFR showed slightly weaker mechanical properties while theoretically, increasing the density of the mixture should show positive effect.

Modulus of rupture (MOR) was the last mechanical test that was used to evaluate the effect of different variables. Results of the MOR test related to L1, L3, and L4 are shown in Figure 10 (c). Figure 11 also shows the flexural stress versus midspan deflection of samples related to L1, L3, and L4 mixtures.

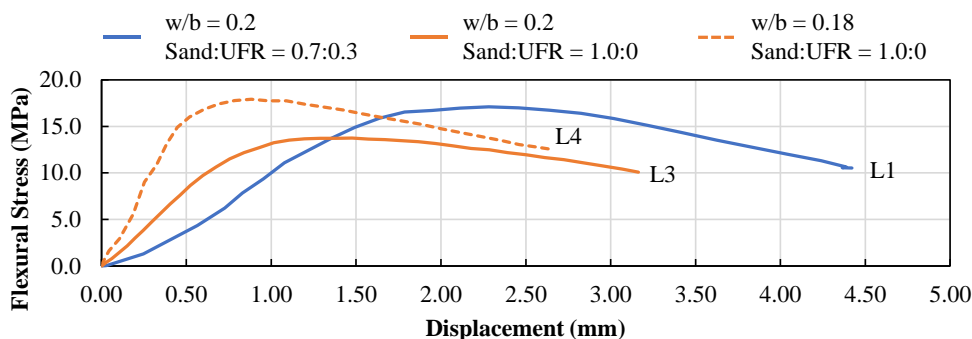


Figure 11: Flexural stress versus midspan displacement curves for samples investigating the effect of w/b and using UFR on the modulus of rupture

5.3 Effect of Moist Curing

The effect of moist curing was investigated on compressive strength, modulus of elasticity, and splitting tensile strength. Figure 12 shows the measured compressive strength and density of both cured and uncured non-proprietary UHPC samples. Results showed that moist curing did not significantly improve the compressive strength and density of samples. Less than one percent improvement was observed for both compressive strength and density of moist cured samples compared to uncured samples. Uncured samples refer to those that were kept in capped cylinders until testing.

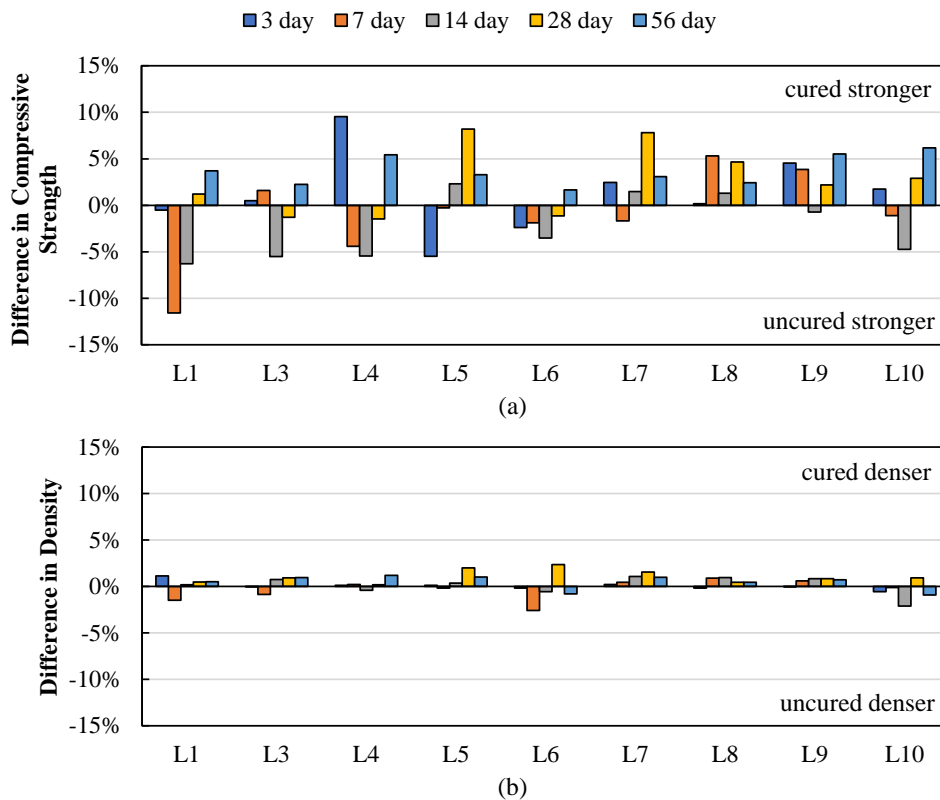


Figure 12: Effect of moist curing on (a) compressive strength and (b) density

Figure 13 shows the results of modulus of elasticity for both moist cured and uncured samples. Results showed on average 7.5% higher modulus of elasticity for moist cured samples compared to uncured samples.

Improvement of modulus of elasticity due to moist curing process was more noticeable for L3 and L5 to L10 mixtures with no UFR and w/b 0.2. For L1 with 30 percent UFR content and L4 with w/b of 0.18, the average measured modulus of elasticity for uncured samples was slightly higher than the average for the cured samples; this is probably due to higher density of L1 and L4 and therefore their lower permeability compared to rest of the mixtures, but still is not clear why moist curing process had negative effect on samples taken from these two mixtures.

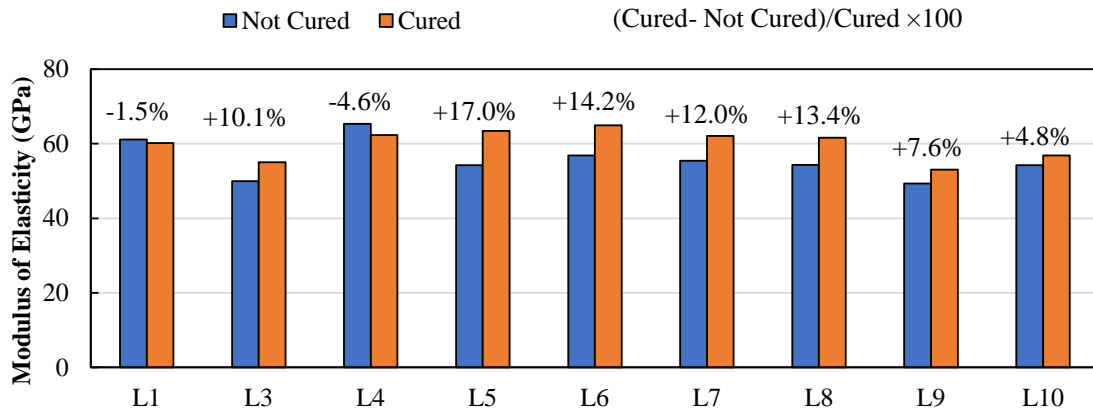


Figure 13: Effect of moist curing on the modulus of elasticity

The effect of moist curing on splitting tensile strength is shown in Figure 14. No clear trend was observed for the effect of moist curing on splitting tensile strength.

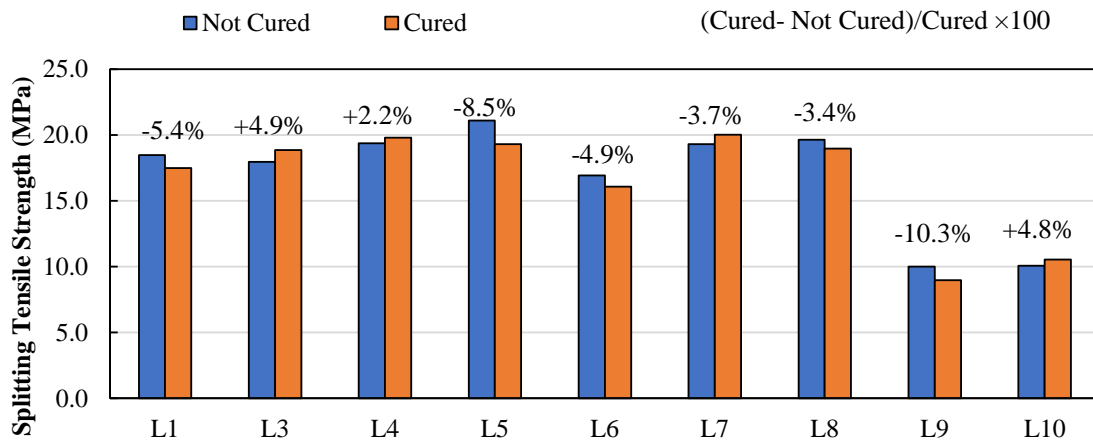


Figure 14: Effect of moist curing on splitting tensile strength

5.4 Bulk Resistivity Test Results

The exceptional mechanical properties of UHPC have made it a good candidate for different applications, but there have been some questions about quantifying the durability of UHPC and its long-term performance. To evaluate the durability of non-proprietary UHPC concrete, bulk resistivity tests were conducted on 101.6 mm by 203.2 mm (4-in. by 8-in.) cylinder samples. This test was performed according to ASTM C1760-12 [25].

For comparison between the non-proprietary UHPC and commercially available UHPC (Ductal®), two additional mixtures were also tested using Ductal® (one with 0 percent fibers, D1, and one with 2 percent

fibers, D2). The average measured bulk resistivity of samples is summarized in Table 5. The measurement was done using the Resipod device and reported values for D1 were based on the maximum measurable value for the Resipod device.

Table 5: Bulk resistivity test results

Mix.	w/b	Sand:UFR	Fiber		Bulk Resistivity (k Ω -cm)					
			Type	Content	3 day	7 day	14 day	28 day	56 day	90 day
L1	0.20	0.7:0.3	OL	2.0%	1.4	2.3	4.9	6.6	12.9	21.9
L3	0.20	1:0	OL	2.0%	4.5	7.0	9.6	15.5	23.8	38.9
L4	0.18	1:0	OL	2.0%	3.1	6.5	9.9	15.5	31.7	56.5
L5	0.20	1:0	HF	2.0%	5.2	8.2	8.3	11.7	23.8	44.9
L6	0.20	1:0	A	1.5%	3.9	5.4	7.5	10.9	16.3	31.9
L7	0.20	1:0	OL	4.0%	2.2	4.2	8.6	11.6	16.2	31.2
L8	0.20	1:0	HF	4.0%	1.4	3.0	7.1	9.4	13.1	25.0
L9	0.20	1:0	Sy	2.0%	9.7	13.7	30.4	59.2	114.8	182.1
L10	0.20	1:0	Sy	1.0%	8.7	11.5	27.2	64.3	137.6	183.4
D1	C-UHPC		OL	0.0%	204.5	204.5	204.5	204.5	204.5	204.5
D2	C-UHPC		OL	2.0%	9.7	15.1	26.2	47.1	78.3	125.3

The typical classification of permeability measurements for bulk resistivity and surface resistivity are shown in Table 6 based on Nugent [35]. Results showed the mixtures containing steel fibers had lower bulk resistivity compared with the mixtures with synthetic fibers but still, all measured bulk resistivity values would be in the very low classification for concrete permeability.

Table 6: Classification of permeability measurements by test method [35]

Classification	RCP (C)	Bulk Resistivity (k Ω -cm)	Surface Resistivity (k Ω -cm)
High	> 4000	< 5	< 12
Moderate	2000 to 4000	5 to 10	12 to 21
Low	1000 to 2000	10 to 20	21 to 37
Very Low	100 to 1000	20 to 200	37 to 254
Negligible	< 100	> 200	> 254

Figure 15 shows the average measured bulk resistivity over time based on different fiber types. Results showed the permeability of UHPC mixtures without fibers or with synthetic fibers was almost negligible. This indicated that the density of the concrete matrix was high enough to create negligible permeability.

Using steel fibers significantly decreased the bulk resistivity, although results would still indicate a very low permeability category. The measured bulk resistivity of mixtures made with steel fibers decreased with increasing fiber contents. Both of these findings show how the presence of steel fibers affects the electrical properties of the UHPC. The alignment of fibers can produce a path for current flow through the specimen with less resistance than the concrete matrix itself, which will decrease the measured resistivity.

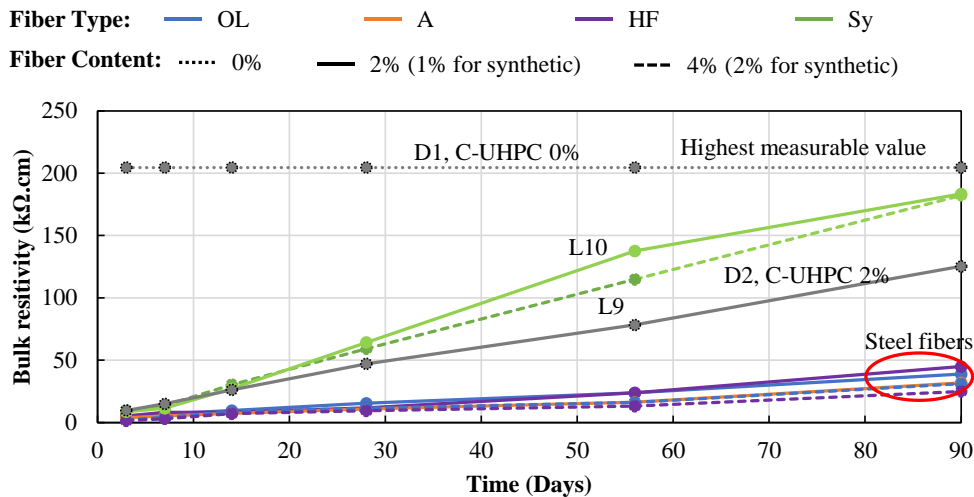


Figure 15: Effect of fiber type and content on bulk resistivity

The effect of w/b and using UFR on the durability of mixtures were also investigated. Figure 16 shows the average measured bulk resistivity over time for L1, L3, and L4 mixtures. As it was expected having lower w/b ratio increased the bulk resistivity of samples (comparing L4 and L4) around 45 percent at 90 days. Results also revealed lower bulk resistivity of the mixture containing UFR (L1) compared to the mixture without UFR (L3); this finding was opposite expectations.

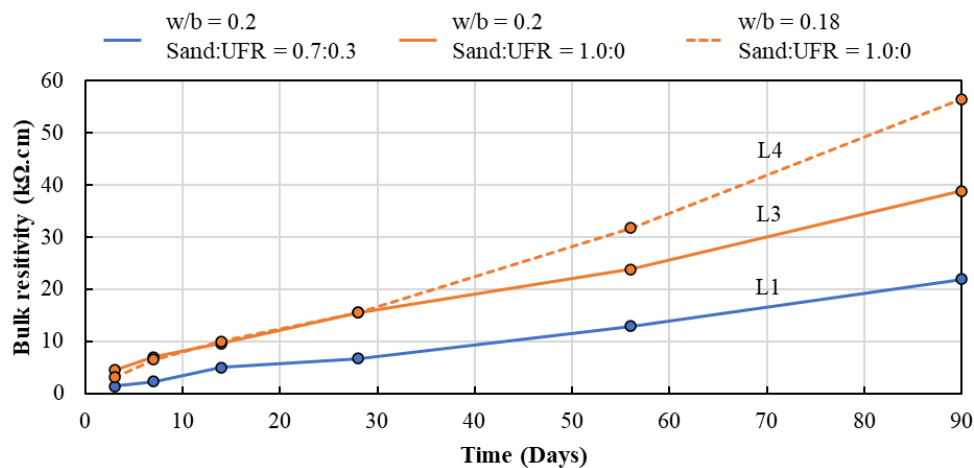


Figure 16: Effect of w/b and UFR on bulk resistivity

6. Conclusion

The widespread use of commercial UHPC mixes has been limited by its relatively high cost, which can be around 20 to 30 times higher than the average price of conventional concrete. This study aimed to investigate the effect of fiber type and content on the mechanical properties of non-proprietary UHPC mixtures with materials from south Florida. This study was conducted through two experimental phases including small-scale trial batches and large-scale batches. Different variables, including fiber type, fiber content, w/b, and UFR content, were investigated.

Some of the significant findings from this research are summarized below:

1. The use of metal fibers with 13-mm length, 0.2-mm diameter, and tensile strength of 2,758 MPa led to the best overall performance of the UHPC (OL and HF fiber). This size fiber was distributed uniformly, and no segregation or clumping issue was observed in mixtures containing these fibers.
2. The use of synthetic fibers led to lower mechanical properties including compressive strength, density, modulus of elasticity, modulus of rupture, and splitting tensile strength. The synthetic fibers had lower tensile strength and modulus than the steel fibers. The synthetic fibers were also more prone to clumping in the mixtures for this project.
3. Increasing the fiber content from 2 to 4 percent, led to similar compressive strength and modulus of elasticity, higher density and tensile strength, and lower bulk resistivity.
4. Lower w/b (0.18 versus 0.2) generally led to higher mechanical properties, although a slightly higher HRWR dosage may be needed to maintain similar flowability.
5. The effect of using UFR with 30% replacement ratio with sand also was studied. Although there was an improved particle packing with the 30% UFR replacement, experimental results did not show significant improvement in all tests. This could be due to the higher required HRWR dosage for mixtures containing UFR, and therefore more investigation is needed to evaluate the effect of using UFR on mechanical properties of non-proprietary UHPC mixtures.
6. Variation in results did not show any specific correlation between time and how moist curing affects the mechanical properties.
7. Metal fibers decreased the bulk resistivity of the samples by creating a path for current flow through the specimen with less resistance than the concrete matrix itself, although all results still were classified in very low permeability category. Samples with synthetic fibers had significantly higher bulk resistivity readings than those with steel fibers.

Acknowledgements

This project was supported by the U.S. Department of Transportation through the Accelerated Bridge Construction University Transportation Center (ABC-UTC). The opinions, findings and conclusions expressed here are those of the author(s) and not necessarily of the sponsor.

7. References

- [1] B. Graybeal, "Ultra-High-Performance Concrete--| Federal Highway Administration," *Accedido Marzo*, vol. 23, 2015.
- [2] M. K. Tadros et al., "Implementation of Ultra-High-Performance Concrete in Long-Span Precast Pretensioned Elements for Concrete Buildings and Bridges," *Precast. Concr. Inst. PCI*, Jan. 2020, doi: <https://doi.org/10.15554/pci.rr.mat-012>.
- [3] K. Wille, A. E. Naaman, and G. J. Parra-Montesinos, "Ultra-High Performance Concrete with Compressive Strength Exceeding 150 MPa (22 ksi): A Simpler Way.," *ACI Mater. J.*, vol. 108, no. 1, 2011.
- [4] M. Berry, R. Snidarich, and C. Wood, "Development of Non-Proprietary Ultra-High Performance Concrete," *Montana Dept. of Transportation Research Programs*, 2017.
- [5] B. Graybeal, "UHPC in the US Highway Infrastructure," *Des. Build. UHPFRC Marseille Fr.*, 2009.
- [6] H. Russel and B. Graybeal, "Ultra-High-Performance Concrete: A State-of-the-Art Report for the Bridge Community. Federal Highway Administration; McLean, VA," 2013.



- [7] J. S. Lawler, M. K. Tadros, M. Lampton, and E. N. Wagner, "Development of Non-Proprietary UHPC for Florida Precast Applications," 2019, vol. 2, no. 1. doi: <https://doi.org/10.21838/uhpc.9689>.
- [8] A. Taфраoui, G. Escadeillas, and T. Vidal, "Durability of the ultra high performances concrete containing metakaolin," *Constr. Build. Mater.*, vol. 112, pp. 980–987, 2016.
- [9] M. Alkaysi and S. El-Tawil, "Effects of variations in the mix constituents of ultra high performance concrete (UHPC) on cost and performance," *Mater. Struct.*, vol. 49, no. 10, pp. 4185–4200, 2016, doi: <https://doi.org/10.1617/s11527-015-0780-6>.
- [10] S. El-Tawil, Y.-S. Tai, J. A. Belcher II, and D. Rogers, "Open-Recipe Ultra-High-Performance Concrete," *Formwork*, p. 33, 2020.
- [11] T. Looney, A. McDaniel, J. Volz, and R. Floyd, "Development and characterization of ultra-high performance concrete with slag cement for use as bridge joint material," *Development*, vol. 1, no. 02, 2019.
- [12] S. El-Tawil, M. Alkaysi, A. E. Naaman, W. Hansen, and Z. Liu, "Development, Characterization and Applications of a Non Proprietary Ultra High Performance Concrete for Highway Bridges," Michigan Dept. of Transportation, 2016.
- [13] M. Berry, "Feasibility of Non-Proprietary Ultra-High Performance Concrete (UHPC) for Use in Highway Bridges in Montana: Phase II Field Application," 2018, [Online]. Available: <https://scholarworks.montana.edu/xmlui/handle/1/15911>
- [14] A. J. Giesler, S. B. Applegate, and B. D. Weldon, "Implementing nonproprietary, ultra-high-performance concrete in a precasting plant," *PCI J.*, vol. 61, no. 6, pp. 68–80, 2016, doi: <https://doi.org/10.15554/pcij61.6-03>.
- [15] B. A. Graybeal, "Development of Non-Proprietary Ultra-High-Performance Concrete for Use in the Highway Bridge Sector: TechBrief," United States. Federal Highway Administration, 2013.
- [16] A. M. Matos, S. Nunes, C. Costa, and J. L. Barroso-Aguiar, "Characterization of non-proprietary UHPC for use in rehabilitation/strengthening applications," in *Rheology and Processing of Construction Materials*, Springer, 2019, pp. 552–559. doi: https://doi.org/10.1007/978-3-030-22566-7_64.
- [17] R. Karim, M. Najimi, and B. Shafei, "Assessment of transport properties, volume stability, and frost resistance of non-proprietary ultra-high performance concrete," *Constr. Build. Mater.*, vol. 227, p. 117031, 2019, doi: <https://doi.org/10.1016/j.conbuildmat.2019.117031>.
- [18] R. Yu, P. Spiesz, and H. Brouwers, "Development of an eco-friendly Ultra-High Performance Concrete (UHPC) with efficient cement and mineral admixtures uses," *Cem. Concr. Compos.*, vol. 55, pp. 383–394, 2015.
- [19] A. Arora, Y. Yao, B. Mobasher, and N. Neithalath, "Fundamental insights into the compressive and flexural response of binder-and aggregate-optimized ultra-high performance concrete (UHPC)," *Cem. Concr. Compos.*, vol. 98, pp. 1–13, 2019.

- [20] E. Shahrokhinasab, T. Looney, R. Floyd, and D. Garber, "Effect of Fiber, Cement, and Aggregate Type on Mechanical Properties of UHPC," *Civ. Eng. J.*, vol. 7, no. 8, pp. 1290–1309, 2021.
- [21] E. Shahrokhinasab and D. Garber, "Development of 'ABC-UTC Non-Proprietary UHPC' Mix," 2021.
- [22] A. Andreasen, "Über die Beziehung zwischen Kornabstufung und Zwischenraum in Produkten aus losen Körnern (mit einigen Experimenten)," *Kolloid-Z.*, vol. 50, no. 3, pp. 217–228, 1930, doi: <https://doi.org/10.1007/bf01422986>.
- [23] D. Dinger and J. Funk, "Predictive process control of crowded particulate suspensions," 1994, doi: <https://doi.org/10.1007/978-1-4615-3118-0>.
- [24] Z. Rong, W. Sun, H. Xiao, and W. Wang, "Effect of silica fume and fly ash on hydration and microstructure evolution of cement based composites at low water–binder ratios," *Constr. Build. Mater.*, vol. 51, pp. 446–450, 2014.
- [25] American Society for Testing and Materials (ASTM), "ASTM C1760-12-Standard Test Method for Bulk Electrical Conductivity of Hardened Concrete," 2012.
- [26] American Society for Testing and Materials (ASTM), "C39/C39M-21 - Standard Test Method for Compressive Strength of Cylindrical Concrete Specimens," 2021.
- [27] American Society for Testing and Materials (ASTM), "C78/C78M-18 - Standard Test Method for Flexure Strength of Concrete (Using Simple Beam with Third-Point Loading)," 2018.
- [28] American Society for Testing and Materials (ASTM), "C469/C469M-14 - Standard Test Method for Static Modulus of Elasticity and Poisson's Ratio of Concrete in Compression," 2014.
- [29] American Society for Testing and Materials (ASTM), "C496/C496M-17 - Standard Test Method for Splitting Tensile Strength of Cylindrical Concrete Specimens," 2017.
- [30] American Society for Testing and Materials (ASTM), "C1437-20 - Standard Test Method for Flow of Hydraulic Cement Mortar," 2020.
- [31] American Society for Testing and Materials (ASTM), "C1856/C1856M - 17 - Standard Practice for Fabricating and Testing Specimens of Ultra-High Performance Concrete," 2017, doi: https://doi.org/10.1520/c1856_c1856m-17.
- [32] American Society for Testing and Materials (ASTM), "C403/C403M - 16 - Standard Test Method for Time of Setting of Concrete Mixtures by Penetration Resistance," 2016.
- [33] American Society for Testing and Materials (ASTM), "C230/C230M - 21 - Standard Specification for Flow Table for Use in Tests of Hydraulic Cement," 2021.
- [34] B. Graybeal, "Design and construction of field-cast UHPC connections.," United States. Federal Highway Administration, 2019.

[35] J. T. Nugent, “Chloride Penetration Resistance of Concrete: An Examination and Comparison of Short-Term Testing Methods,” Thesis, Jan. 2020.



This work is licensed under a Creative Commons Attribution Non-Commercial 4.0 International License.